

Microstructures in a ternary eutectic alloy: devising metrics based on neighbourhood relationships

A Dennstedt¹, A Choudhury², L Ratke³, and B Nestler⁴

¹Institut für Materialphysik im Weltraum, Deutsches Zentrum für Luft- und Raumfahrt (DLR), 51170 Köln, Germany

²Indian Institute of Science, Department of Materials Engineering, 560012 Bangalore, India

³Institut für Werkstofforschung, Deutsches Zentrum für Luft- und Raumfahrt (DLR), 51170 Köln, Germany

⁴Institut für Angewandte Materialien, Karlsruhe Institut für Technologie, 76131 Karlsruhe, Germany

E-mail: ¹anne.dennstedt@gmx.com, ²abhiknc@gmail.com, ³lorenz.ratke@dlr.de, ⁴britta.nestler@kit.edu

Abstract. Ternary eutectics, where three phases form simultaneously from the melt, present an opportunity to study the fundamental science of microstructural pattern formation during the process of solidification. In this paper we investigate these phenomena, both experimentally and by phase-field simulations. The aim is to develop necessary characterisation tools which can be applied to both experimentally determined and simulated microstructures for a quantitative comparison between simulations and experiments. In SEM images of experimental cross sections of directionally solidified Ag-Al-Cu ternary eutectic alloy at least six different types of microstructures are observed. Corresponding 3D phase-field simulations for different solidification conditions and compositions allow us to span and isolate the material parameters which influence the formation of three-phase patterns.

Both experimental and simulated microstructures were analysed regarding interface lengths, triple points and number of neighbours. As a result of this integrated experimental and computational effort we conclude that neighbourhood relationships as described herein, turn out to be an appropriate basis to characterise order in patterns.

1. Introduction

During solidification of a eutectic melt several solid phases appear at the same time while no melt will be left. In the case of binary eutectics two phases are created. They can be arranged as lamellae or as fibres in a matrix. Which pattern will be created depends on the eutectic composition. In the case of ternary eutectics three phases are created. As a result many more arrangements are possible. Lewis et al. published a sketch showing five types of ternary eutectics [1] that were before verbally listed by Ruggiero and Rutter [2]. However, in reality ternary eutectics are much more complex as shown in this sketch ([3, 4, 5, 6, 7] and refs. therein) and their structures generally fail to be describable by the simple geometrical approaches [8].

The system Ag-Al-Cu provides one ternary eutectic at a composition of 18.1 at% Ag, 69.1 at% Al and 12.8 at% Cu [9]. After solidification of such a melt the phase fractions change due to solid state reactions to almost equal volume fractions of the three phases α -Al, Ag₂Al and Al₂Cu [4]. Here, we describe different microstructures observed in directionally solidified ternary



eutectic Ag-Al-Cu alloy and determined neighbourhood relationships both in these experimental images as well as in images of simulated microstructures.

2. Experimental procedure and simulation technique

Ag-Al-Cu alloys of eutectic composition were cast into stainless steel moulds. Subsequently, rods were machined to fit the ARTEMIS facility. The ARTEMIS facility [10] was used to perform directional solidification with velocities of 0.08 to 3.8 $\mu\text{m/s}$ and applied gradients of 1.5 to 6.2 K/mm. Experiments with a single solidification velocity as well as experiments with two or three different solidification velocities were performed in one run with one sample. Cross sections of the directionally solidified rods were prepared using standard metallographic procedures. Scanning electron microscope (SEM) images were collected using the backscattered mode to show microstructures of this ternary eutectic. The contrast between the three phases is excellent: white represents the Ag_2Al phase, black the solid solution $\alpha\text{-Al}$, and gray the Al_2Cu phase. Comparing all images different microstructures are differentiable. Six images showing characteristics of these microstructures were chosen to discuss characteristics of these microstructures in ternary Ag-Al-Cu alloy.

The first phase-field simulations of this alloy were performed by Apel et al. (Chapter 29 in [11]). In the present analysis our aim is to investigate the material parameters and conditions which lead to the selection of the different patterns in a ternary eutectic alloy. Phase-field simulations were performed on the basis of the quantitative phase-field model presented in [12]. However, the thermodynamic description of the bulk free-energy densities is modified wherein information from the CALPHAD databases [9] was incorporated by forming simplistic parabolic free energies, with local thermodynamic extrapolation of the equilibrium chemical potential and the equilibrium solidus and liquidus compositions along the tie-lines given by the eutectic compositions. The modification ensures an easier and efficient coupling with the databases than what was previously used in the ideal energy solution model in [12]. The entire description ensures that the equilibrium compositions of phases and the slopes of the liquidus are exactly mapped, correspondingly as in the information from the thermodynamics databases, near the ternary eutectic point. Additionally the variation of the composition as a function of the chemical potentials is derived accurately until second order in $\mu - \mu_{eq}$, (μ being the chemical potential and μ_{eq} the equilibrium value) which is a consequence of the actual free-energy densities from the databases being approximated by second-order polynomials. This ensures that the Gibbs-Thomson coefficient which at leading order comprises of the ratio of the surface energies and the second derivatives of the free-energy w.r.t composition is accurately represented. A detailed overview can be found in a recent publication [15].

For the comparison with the present experimental results, wherein the volume fractions differ from those predicted from the CALPHAD databases [9] because of kinetic reasons, we shift the ternary eutectic point corresponding to the volume fractions achieved in experiments, while keeping all the liquidus and solidus slopes as derived from the thermodynamic databases. This is essential since volume fractions are a key parameter influencing pattern formation. The simulated microstructures are thereafter analysed in a comparable way like the experimental microstructures.

3. Results and discussion

Comparing all cross sections at least six different types of microstructures were observed. Figures 1a to 1f show examples for these structures.

An aligned structure (figure 1a) was detected that is called ladder or brick-like structure and which is expected for slowly solidified ternary Ag-Al-Cu alloy [3, 4, 13]. Therein two intermetallic phases Ag_2Al and Al_2Cu alternate in a row and thus one could imagine them as one lamella consisting of two sub-lamellae. In between the $\alpha\text{-Al}$ phase separates as parallel lamellae the

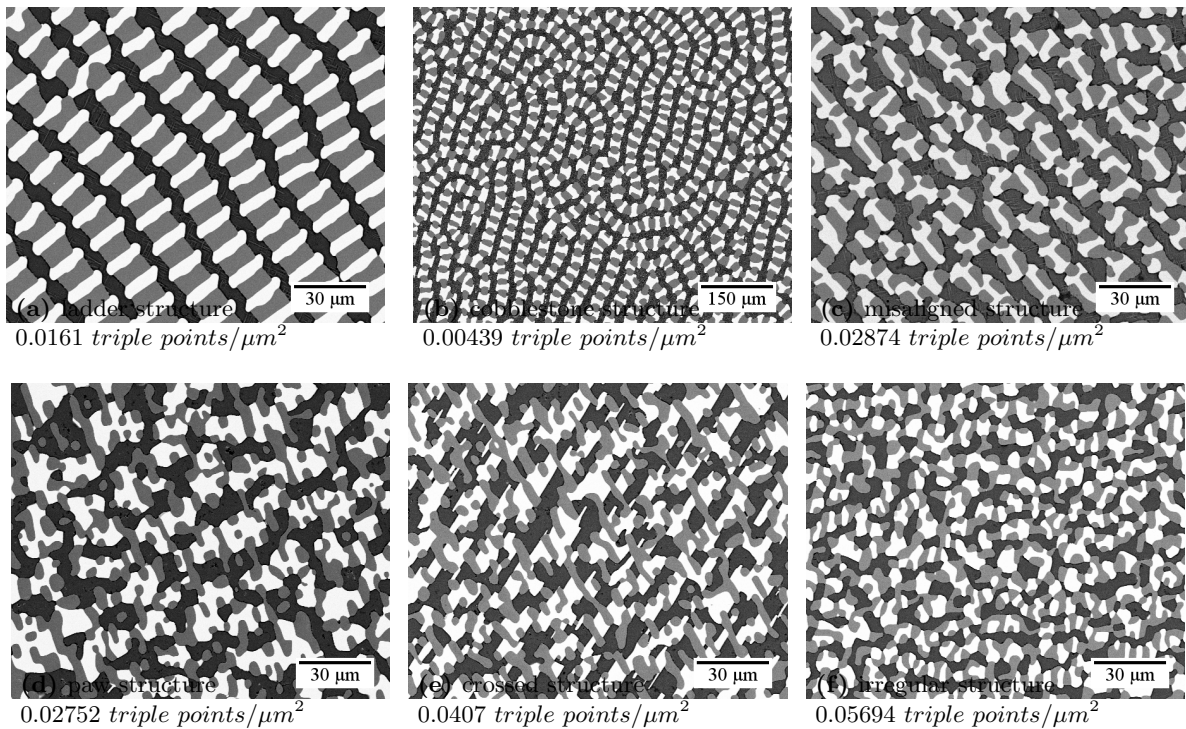


Figure 1. SEM images of Ag-Al-Cu alloy solidified with (a) $0.39 \mu\text{m/s}$ and 6.2 K/mm ; (b) $0.08 \mu\text{m/s}$ and 2.2 K/mm ; (c) $0.72 \mu\text{m/s}$ and 3.3 K/mm ; and (d) to (f) $1.9 \mu\text{m/s}$ and 3.2 K/mm . White = Ag_2Al , gray = Al_2Cu , black = Al.

intermetallic super-lamellae. In contrast thereto a structure was observed showing bended α -Al lamellae or particles (figure 1b). The intermetallic superlamella still shows alternating Ag_2Al and Al_2Cu phases. We called this structure a cobblestone (pavement) structure. Alternatively, in a third microstructure (figure 1c), the α -Al lamellae still develop elongated particles which are arranged in parallel and can be identified as lamellae. However, the intermetallic lamellae are internally unaligned. On the basis of the brick-like structure we called this microstructure a misaligned structure. The microstructures shown in figure 1d to 1f were detected in a single cross section in different regions, and corresponding regions were also detected in cross sections later in the solidification. The reasons for these different microstructures are until now not known. In the microstructure in figure 1d the Al_2Cu particles can be thought as threaded phase particles. The Ag_2Al phase is arranged in between the Al_2Cu particles in such a way that the α -Al phase still is in lamellae and thus the different Ag_2Al shapes sometimes mimic an H or a doubled H. If there are many more than four neighbored Al_2Cu particles attached to a single Ag_2Al particle the shape of this arrangement resembles an animal climbing on a tree. Thus, this microstructure is called a paw structure. Figure 1e shows not only elongated Al_2Cu particles but also elongated Ag_2Al particles. These elongations are oriented in different directions, and we called the microstructure a crossed structure. After all, a further microstructure was observed where all three phases are placed in an unaligned and irregular way (figure 1f). The intermetallic phases Ag_2Al and Al_2Cu are irregularly connected. Thus a higher number of intermetallic neighbours is possible and the particles of the α -Al phase are smaller and curved in comparison to the more ordered structures.

We analysed each image concerning triple point density, number of particles per image area

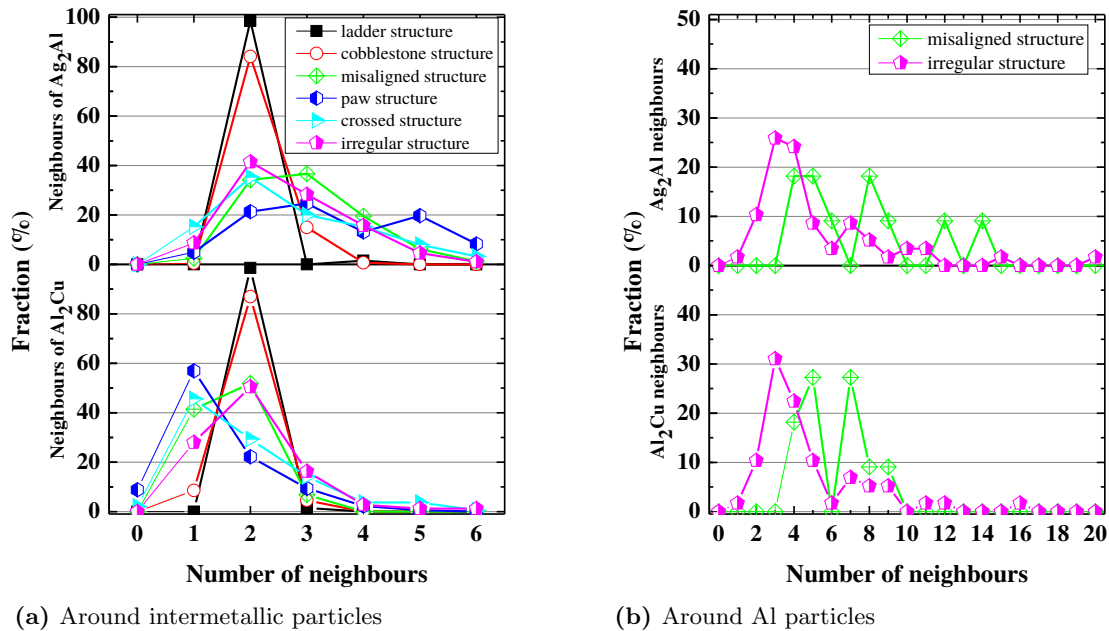


Figure 2. Results from experimental microstructures: fraction of particles with (a) up to 6 intermetallic neighbours around the intermetallic particles, and (b) up to 20 neighbours around the Al particles in misaligned and irregular structure.

as well as size and perimeter of the particles. These parameters strongly dependent on the solidification conditions. As known already [14], larger particles are observed for solidifications with lower solidification velocities. This means that not only size but also perimeter of the particles increases with decreasing solidification velocity as well as the number of particles and triple point density decrease. Because microstructures shown here were not obtained with same solidification velocity a comparison of all microstructures using these four parameters is not useful. However, triple point densities determined on the images are written below the single images 1a to 1f. Different values are observed for paw, crossed and irregular structure even so they were formed under the same solidification conditions. Thus, the triple point density depends not only on solidification parameters but also on the microstructure created.

A parameter not depending on solidification velocity is the number of neighbours of the intermetallic particles [4]. However, we detect clear differences between the different microstructures. Figure 2a shows in the upper part how many of the Ag_2Al particles feature 0, 1, 2 or more Al_2Cu neighbours. In the lower part of this figure the Al_2Cu particles were analysed. In the ladder structure nearly all intermetallic particles have two intermetallic neighbours (figure 2a). In the cobblestone structure the fraction of intermetallic particles with two neighbours decreased. The other microstructures show an even further decreased fraction of intermetallic particles with two neighbours. As a consequence of this more Ag_2Al particles show more than 2 neighbours whereas more Al_2Cu particles show less than 2 neighbours.

In figure 3 the fraction of Ag_2Al particles with two Al_2Cu neighbours is plotted against the fraction of Al_2Cu particles with two Ag_2Al neighbours. The fraction of Ag_2Al particles is mostly similar to the fraction of Al_2Cu particles thus all points are plotted near a line $x=y$. The most ordered structure is the ladder structure and it's point is plotted most far away from the point of

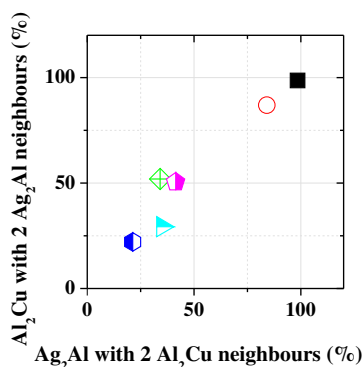


Figure 3. A fraction-fraction plot for the experimental microstructures.

origin. The second in this row is the cobblestone structure showing fractions of more than 80% with two neighbours. The points for misaligned and irregular structure (figure 1c and 1f) are plotted near each other, but a comparison of the images shows that these two microstructures are not the same. The distributions of intermetallic neighbours around the intermetallic particles are very similar (figure 2a). However, the distributions of intermetallic neighbours around the α -Al particles differ strongly (fig.2b). In the case of the misaligned structure the Al particles feature more neighbours compared to the α -Al particles in the irregular structure.

Figures 4 shows results of a 3D phase-field simulation resulting in a microstructure similar to a brick-like structure. The figures from left to right highlight the various stages during the early stage of solidification until a uniform microstructure is achieved.

We tiled the simulated images to analyse also the larger particles touching the image borders. Similar to neighbour relationships in the experimental microstructures the fraction of Ag₂Al particles as well as of Al₂Cu particles with two intermetallic neighbours is changing, resulting to high fractions in the case of more order (figure 5). The analysis tools developed enable the quantification of the increase in order of the simulated microstructure with increase in solidification time. Additionally, the apparent similarity between the ladder-structure and the simulation images is adequately captured by the analysis tools. While there are certain small differences between the neighbour fractions of 1 and 3 neighbours between the simulations and the experiments, it is possible that with increase in the simulation box-size, that an improved statistics are possible with reduced differences.

While, we do not present a more thorough analysis into the actual mechanisms of pattern selection and the influence of the several material and process parameters since it is outside the scope of the present paper, we will be presenting a more detailed analysis in a forthcoming publication [16], where we characterize the influence of solid-liquid interfacial energies and volume fractions of the solids on pattern formation during three-phase growth.

4. Conclusions

In this paper 6 different microstructures observed in directionally solidified ternary eutectic Ag-Al-Cu alloy experiments are described. We describe neighbourhood relationships that allow us to characterise order and thereby quantitatively distinguish each of the observed microstructures. The developed analysis tools are generally applicable even for characterizing simulated microstructures. Phase-field simulations are utilised to understand early stage pattern formation resulting in the development of one of the experimental microstructures which is described as the ladder-structure in the paper. Quantitative investigation with the help of analysis tools show the increasing order in the simulated microstructure with increasing

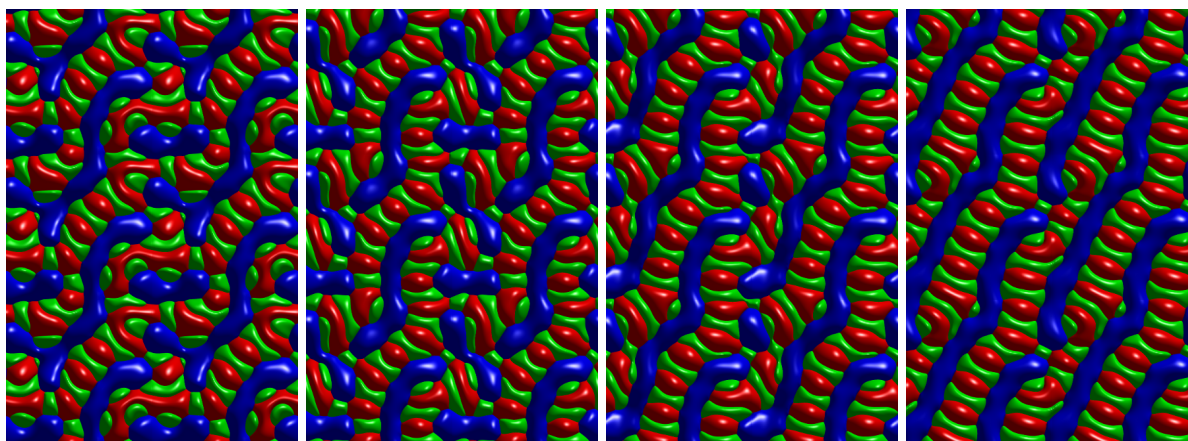


Figure 4. Simulation images for ternary eutectic alloy showing microstructure at different time steps (2*3 tiles)(increasing time, from left to right). Green = Ag_2Al , red = Al_2Cu , blue = Al.

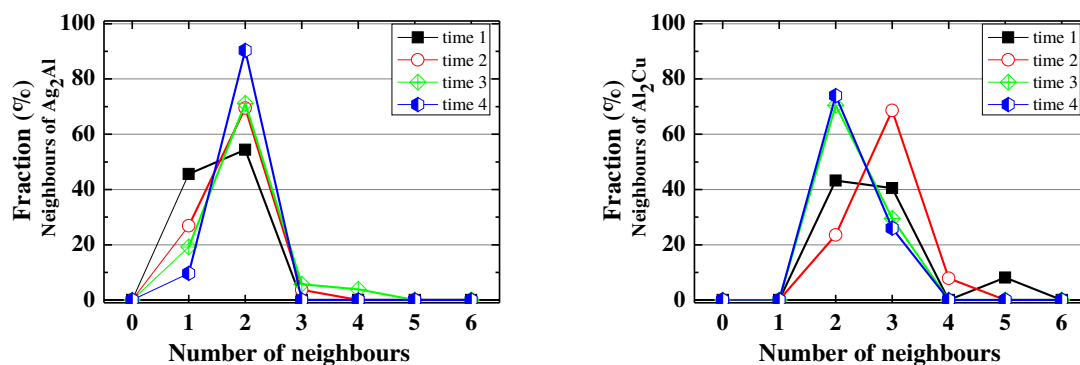


Figure 5. Results from simulated microstructures: fraction of particles with up to 6 intermetallic neighbours around the intermetallic particles.

solidification time, and additionally confirms the resemblance between the simulated and experimental microstructure to a good deal of accuracy.

Acknowledgment

The authors gratefully acknowledge the financial support by the Deutsche Forschungsgemeinschaft under contract numbers RA537/14-2 and NE822/14-2.

References

- [1] Lewis D, Allen S, Notis M, Scotch A 2002 *J. Electron. Mater.* **31** 161
- [2] Ruggiero M A, Rutter J W 1997 *Mater. Sci. Technol.* **13** 5
- [3] Genau A and Ratke L 2011 *IOP conf. Ser.: Mater. Sci. Eng* **27** 012032
- [4] Genau A and Ratke L 2012 *Int. J. Mat. Res.* **103** 469
- [5] Dennstedt A and Ratke L 2012 *Trans Indian Inst Met* **65** 777
- [6] Dennstedt A, Ratke L 2013 *Metallogr. Microstruct. Anal.* **2** 140
- [7] Hawksworth A, Rainforth W M, Jones H 1998 *Scr. Mater.* **39** 1371
- [8] Himemiya T and Umeda T 1999 *Mater. Trans. JIM* **40** 665
- [9] Witusiewicz V T, Hecht U, Fries S G and Rex S 2005 *J. Alloys Compd.* **387** 217
- [10] Alkemper J, Sous S, Stöcker C, Ratke L 1998 *J Cryst. Growth* **191** 252

- [11] Apel M, Böttger B, Witusiewicz V T, Steinbach I 2004 *Solidification and Crystallization*, WILEY-VCH Verlag GmbH & Co. KGaA, Weinheim ISBN: 3-527-31011-8
- [12] Choudhury A, Nestler B Phys. Rev. E **85** 021602
- [13] McCartney D G, Hunt J D, Jordan R M 1980 *Metall. Mater. Trans. A* **11** 1243
- [14] Kurz W, Fisher D J 1989 *Fundamentals of Solidification* (Trans Tech Publications Ltd, Switzerland)
- [15] Choudhury A, Kellner M, Nestler B Current Opinion in Solid-State and Materials Science *Accepted article*
- [16] Choudhury A, Dennstedt A, Ratke L, Nestler B, Physical Review E *Article in review*